# Curing of Bisphenol M Dicyanate Ester under Nanoscale Constraint

**Qingxiu Li and Sindee L. Simon***

*Department of Chemical Engineering, Texas Tech University, Lubbock, Texas 79409*

*Received September 25, 2007; Revised Manuscript Received December 3, 2007*

ABSTRACT: Nanoscale constraint is known to have a significant impact on the thermal properties of materials. Although thermosetting resins have been cured in the presence of nanoparticles and nanotubes, cure of thermosetting resins under the well-defined nanoscale constraints imposed by controlled pore glass (CPG) or similar matrices has not been previously documented. In this work, we investigate the isothermal curing under nanoscale constraint of a thermosetting resin, bisphenol M dicyanate ester (BMDC), which trimerizes to form a polycyanurate network material. Differential scanning calorimetry is used to monitor the evolution of the glass transition temperature ($T_g$) and the conversion during cure as a function of the diameter of the silanized control pore glass matrix which is used for confinement. A $T_g$ depression is observed for both the bisphenol M dicyanate ester monomer and the polycyanurate networks; the depression is only a few degrees for the monomer, whereas a 56 K depression is observed for the "fully cured" network in 11.5 nm pores. The nanoscale constraint is also found to strongly increase the rate of cure of bisphenol M dicyanate ester, but it does not affect the normalized $T_g$ vs conversion relationship. The appearance of a secondary $T_g$ above the primary $T_g$ in the smaller pores and the associated length scale are discussed.

## Introduction

Since the pioneering work by Jackson and McKenna in the early 1990s,[1,2] numerous studies have reported that the thermal properties of materials are affected under nanoscale constraint.[3−10] The behavior of low-molecular-weight and polymeric glass formers confined in nanoporous matrices has been extensively examined.[2−10] The glass transition temperature, $T_g$, is found to decrease, increase, or remain unchanged with size scale depending on the glass former, nanoconfinement methodology, surface interactions, and measuring technique.[2−9]

Although the effects of nanoconfinement on the glass transition temperature of low-molecular-weight and thermoplastic polymeric glass formers have been well studied, the effects of nanoconfinement on thermosetting network polymers have only been examined by one research group[11] in spite of the importance of the properties of nanoconfined thermosetting polymers in the microelectronic industries. In that only work, the glass transition temperature of the microtome-sliced epoxy thin film was found to decrease with film thickness, and a $T_g$ depression of 15 K was observed for a 40 nm thin film.[11] On the other hand, no prior studies have examined the effect of curing thermosetting resins under nanoscale constraint, although considerable efforts have focused on the curing of thermosetting resins in the presence of nanoparticles[12−24] and nanotubes[25−33] and the influence of nanoparticles and nanotubes on the glass transition temperature of the resin.[12−14,16,17] For epoxy/SiC, epoxy/silica, epoxy/organoclay, and epoxy/cyanate ester/organoclay nanocomposites, the glass transition temperature of the polymer decreases with increasing nanoparticle loading;[12−14,16] however, when the nanosilica is directly prepared in epoxy, the $T_g$ of the polymer increases with nanoparticle concentration presumably because of chemical bonding between the nanosilica and the secondary hydroxyl groups on the epoxy molecules.[17]

Cure of thermosetting resins under nanoscale constraint is the inverse problem of thermosets cured in the presence of nanoparticles and nanotubes, and close relevance exists between these two systems as evidenced by the simulation and experimental work.[34,35] Recently, the molecular dynamics simulations by Starr et al. reveal a similarity between nanoparticle-filled systems and ultrathin polymer films.[34] The experimental work on polystyrene/silica nanocomposites by Bansal et al. further demonstrates that the thermomechanical properties of polymer nanocomposites are similar to thin films.[35] Analogous to ultrathin films, the glass transition temperature of the polymer in the nanocomposites decreases with deceasing interparticle spacing if strong interactions are not present between the polymer and the nanoparticles or nanotubes, whereas it increases in the presence of strong interactions.[36,37]

Among various types of thermosetting resins, cyanate esters are one important group with unique properties such as high glass transition temperatures, low dielectric loss, and relatively high fracture toughness; therefore, these resins are widely used in the electronic and aerospace composite industries.[38] In this work, we investigate the isothermal cure of bisphenol M dicyanate ester to form polycyanurate under the well-defined nanoscale constraint of controlled pore glasses (CPGs) as a function of nanopore size. The bulk cure kinetics of this particular dicyanate ester monomer are well described by a second-order plus second-order autocatalytic reaction model:[39]

$$\frac{dx}{dt} = k(1-x)^2(x+b) \tag{1}$$

where $x$ is conversion and $t$ is cure time. The Arrhenius rate constants, $k$ and $kb$, for the second-order autocatalytic and second-order reactions, respectively, have different activation energies. This equation, coupled with the DiBenedetto[40] relationship for $T_g$ vs conversion, is able to describe the evolution of $T_g$ during cure in the bulk system.[39] The DiBenedetto equation is given by the following:

$$T_g^* = \frac{T_g - T_{g0}}{T_{g\infty} - T_{g0}} = \frac{\lambda x}{1-(1-\lambda)x} \tag{2}$$

* Corresponding author. E-mail: Sindee.Simon@ttu.edu.

10.1021/ma702144b CCC: $40.75 
Published on Web 01/25/2008

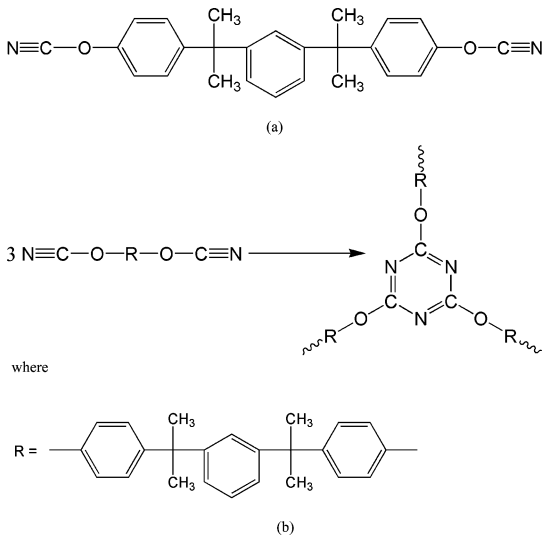


**Figure 1.** Chemical structure of (a) bisphenol M dicyanate ester and (b) the trimerization reaction of bisphenol M dicyanate ester.

where $T_g$* is the dimensionless glass transition temperature, $T_{g0}$ is the $T_g$ of the uncured monomer, $T_{g\infty}$ is the maximum $T_g$ obtained experimentally for the "fully cured" material, and $\lambda$ is a structure-dependent parameter. We note that highly cross-linked materials such as dicyanate esters cannot reach 100% conversion due to topological constraints—hence, "fully cured" refers to the maximum achievable conversion. In addition to the cure kinetics, the development of the network structure of bisphenol M dicyanate ester during cure is well understood, consisting of the principal trimerization reaction in addition to a monomer cyclization side reaction.[41] Furthermore, cyanate esters can cure with or without the presence of catalyst, the latter of which we exploit in the current study since using a single-component system prevents problems associated with the partitioning of components in the nanopores that can occur in multicomponent systems. For the uncatalyzed system, the resin can also easily imbibe in the nanopores at an elevated temperature without undergoing significant degree of cure.

## Experimental Methodology

**Materials.** The thermosetting resin used in this study is bisphenol M dicyanate ester (BMDC, trade name RTX-84921 from Hi-Tek Polymers, Louisville, KY). The chemical structure of bisphenol M dicyanate is shown in Figure 1a; the principal trimerization curing reaction and the polycyanurate triazine cross-linking structure are shown in Figure 1b. The nominal molecular weight of the monomer is 396 g/mol. No catalyst is used in this study in order to allow the liquid monomer to be imbibed into the nanopores above its melting temperature of 68 °C[42] without undergoing a significant degree of curing. The bulk monomer has a glass transition temperature of −28 °C, but it is used in solid form due to crystallization upon prolonged storage in the refrigerator at around −10 °C. The density of the supercooled liquid monomer is ∼1.14 g/cm$^3$ at 25 °C, and the Brookfield viscosity of the liquid is 0.5 Pa s at 65 °C, both as provided by Huntsman, another manufacturer which supplies BMDC monomer in liquid form. The density of "fully cured" polycyanurate at 25 °C is 1.39 ± 0.14 g/cm$^3$ as measured by means of Archimedes' principle.

The nanoconfinement mediums used are four controlled pore glasses (CPGs, produced from borosilicate glass by Millipore, Billerica, MA) with pore sizes ranging from 11.5 to 287.8 nm. All of the controlled pore glasses have a mesh size of 120/200 or 74−125 $\mu$m, and the bulk density of the particles is ∼300 g/L as provided by the manufacturer. The specifications of the controlled pore glasses are listed in Table 1 also as provided by the manufacturer. To eliminate the effect of hydroxyl groups on the CPG surfaces, the controlled pore glasses were treated as follows: the raw controlled pore glasses were first cleaned by immersing in 69.7% nitric acid at ∼100 °C for 10 h, rinsed well with distilled water, and dried at 285 °C for 24 h under vacuum. The cleaned controlled pore glasses were then derivatized with hexamethyldisilazane to convert the surface hydroxyl groups to trimethylsilyl groups following the procedure reported in the literature.[1] The silanization treatment does not significantly affect the pore size.[43] The silanized CPGs are stored in a desiccator before use.

**DSC Measurements.** A Mettler-Toledo differential scanning calorimeter DSC823e with a Julabo FT100 intracooler and nitrogen purge gas was used for calorimetric measurements. Controlled pore glass with weight ranging from 6.79 to 21.12 mg was loaded into 100 $\mu$L DSC pans followed by the BMDC monomer with a sample size ranging from 5.36 to 12.28 mg. The DSC pans were sealed under nitrogen atmosphere. The order of sample loading is important for the complete penetration of the monomer into the controlled pore glass, which was accomplished at 100 °C. The controlled pore glasses are all underfilled and the fullness ranges from 53% to 98% to ensure that all of the resin is imbibed in the pores. The glass transition temperature is found to be the same, within the error of the measurements, independent of degree of pore fullness for the materials studied. For example, for the BMDC monomer confined in the smallest 11.5 nm pores, nine samples with fullness ranging from 69% to 98% were measured; no trend was observed with respect to fullness, and the standard deviation of the $T_g$ measurements was 1.6 °C. For the "fully cured" polycyanurate network confined in the smallest pores, similar results were obtained from four samples with fullness ranging from 69% to 82%, although the standard deviation in this case was larger at 4.5 °C, but again, no trend in the data was observed with respect to pore fullness; the larger standard deviation for $T_g$ of the "fully cured" materials is due to a smaller step change in the heat capacity at $T_g$ ($\Delta C_p$) compared to the monomer and the presence of a second $T_g$ approximately 25 K higher.

Prior to the DSC measurements, the monomer was imbibed into the CPGs at 100 °C, as already indicated. The monomer was allowed to imbibe into the CPGs for 3 min; then $T_g$ was measured, followed by an additional 10 h at 100 °C to ensure complete imbibement. Negligible cure (<1%) occurs at 100 °C after 10 h for the monomer under nanoconfinement as confirmed by the calculation of the conversion change and also as evidenced by the slight increase (<1 K) of the primary glass transition temperature of the monomer. The ability of the resin to be imbibed in a matter of minutes at 100 °C is corroborated by the model of Huber et al.,[44] which predicts that the imbibition velocity $v_i$ is a function of the resin surface tension $\sigma$, the resin viscosity $\eta$, and the contact angle $\theta$, as shown in eq 3:

$$v_i = \frac{\sigma}{\eta}\cos(\theta) \tag{3}$$

For bisphenol M dicyanate ester monomer, $\sigma$ is assumed to be 36 mN/m at 100 °C based on the literature values of similar dicyanate ester and epoxy resins of ∼40 mN/m at 20 °C[45−48] and a temperature coefficient of −0.05 mN/(m K).[49] The viscosity of BMDC at 100 °C is calculated to be 0.015 Pa s based on the "universal" Williams−Landel−Ferry (WLF) equation,[50] the $T_g$ of the monomer, and the viscosity reported by the manufacturer at 65 °C. The contact angle $\theta$ of bisphenol M cyanate ester on the silanized borosilicate glass at room temperature is 45 ± 2° as measured by us on a Ramé-Hart goniometer, and it is expected to decrease by at least 30% at 100 °C on the basis of the temperature dependence of the contact angle of another thermosetting resin reported in the literature.[51] Thus, the imbibement velocity of bisphenol M dicyanate ester in the controlled pore glasses is determined to be ∼2.1 m/s at 100 °C. The total length of the pores inside the particle ($l$), shown in Table 1, is calculated from the bulk density of CPG particle, the particle size, and either the specific pore volume or the specific surface area. Assuming that the diffusion length is half of the total length of the pores inside the particle (a

**Table 1. Specifications of Controlled Pore Glasses**

| product name | mean pore diam (nm)[a] | pore diam distribn (%)[b] | specific pore vol ($cm^3/g$)[a] | specific surface area ($m^2/g$)[c] | total pore length inside the particle (m/particle)[d] | total pore length inside the particle (m/particle)[e] |
|---|---|---|---|---|---|---|
| CPG00120B | 11.5 | 7.3 | 0.49 | 119.5 | 1447 | 1015 |
| CPG00240B | 24.6 | 7.7 | 0.83 | 79.6 | 536 | 316 |
| CPG01000B | 110.6 | 3.6 | 1.06 | 25.0 | 167 | 90 |
| CPG3000B | 287.8 | 5.3 | 1.06 | 8.6 | 34 | 22 |

[a] Determined by mercury intrusion method. [b] Analyzed by ultrasonic sieving method. [c] Measured by nitrogen adsorption method. [d] Based on the specific pore volume. [e] Based on the specific surface area.

gross overestimate), the imbibement time of BMDC monomer in the CPGs is predicted to be less than 6 min in the smallest pores at 100 °C and less than 1 min in the largest pores at the same temperature. We note that Park and McKenna similarly suggested that polystyrene/*o*-terphenyl (PS/*o*-TP) solutions were drawn into the silanized controlled pore glasses via capillary force.[4] The imbibition model thus corroborates our finding that the resin is imbibed in the controlled pore glasses on the order of a few minutes or less.

Two types of DSC measurements were performed: one to measure the glass transition temperature ($T_g$) as a function of cure time during isothermal cure at 180 °C and the other to measure the residual heat of reaction to determine the relationship between the glass transition temperature and conversion. We perform the DSC measurements on heating after cooling at a given rate. Such measurements are analyzed to give the limiting fictive temperature ($T_f'$) by the method proposed by Moynihan et al.:[52,53]

$$\int_{T_f'}^{T\gg T_g} (C_{pl} - C_{pg})\,dT = \int_{T\ll T_g}^{T\gg T_g} (C_p - C_{pg})\,dT \qquad (4)$$

where $C_{pl}$ and $C_{pg}$ are the liquid and glass heat capacities, respectively, and $C_p$ is the apparent heat capacity of the material measured by DSC. Accordingly, the heat flow of the DSC curve was integrated, and the limiting fictive temperature was determined by the interception of the extrapolation of the liquid enthalpy line and the glassy enthalpy line. The $T_f'$ values thus measured are approximately equal (within ~1 K) to the glass transition temperature ($T_g$) that would be obtained on cooling at the same rate.[54−56] Consequently, although $T_f'$ is measured, we call this value the glass transition temperature ($T_g$) in the remainder of the text.

For the measurement of the glass transition temperature of the monomer, the sample was first held at 100 °C for 3 min to remove the crystallites in the BMDC monomer and to imbibe the material in the pores; then it was cooled to −60 °C at 10 K/min. The glass transition temperature (i.e., $T_f'$) of the monomer was obtained on the following heating run at 10 K/min. As already mentioned, to ensure complete penetration of the monomer into the nanopores, the sample was then subsequently held at 100 °C for 10 h, and the glass transition temperature was remeasured on heating at 10 K/min after cooling to −60 °C at 10 K/min. We note that in the DSC heating scan for the monomer confined in the 11.5 nm pores there were several events that could be interpreted as step changes associated with $T_g$. In order to ascertain whether or not these were indeed $T_g$s, the sample was annealed for 2 h at a temperature ~5 K below each event to determine whether an endothermic enthalpy overshoot (or annealing peak) could be obtained, indicating that the event was indeed a $T_g$. Two of the events disappeared on annealing, suggesting that they may result from residual stress instead of being glass transitions. Similar calorimetric events were also discovered for benzoin isobutyl ether confined in the silanized porous glasses with pore diameter of 5 nm or smaller by Donth and co-workers; in that work, the events were termed as "structural peaks".[57]

After complete imbibement, the monomer was cured at 180 °C for various times up to 8 days, and the glass transition temperature was measured periodically at 10 K/min upon heating to 180 °C after cooling at 10 K/min to −60 °C. One sample was thus used to obtain glass transition temperature vs cure time for each system in this type of measurement, and at least three replicate samples were cured to obtain the ultimate glass transition temperature ($T_{g\infty}$). Because of the long cure times involved for the uncatalyzed system, negligible cure occurs during the scans used to periodically obtain $T_g$. For samples that vitrified during cure, large endothermic aging peaks were observed, and the method in the paper by Simon and Gillham[39] was applied to eliminate the effect of aging on $T_g$. For samples with high $T_g$ values (≥170 °C), the scan was performed up to 210 °C for the nanoconfined samples and to 220 °C for the bulk sample. We note that generally thermosetting polymers are cured at temperatures at or above their ultimate $T_g$ ($T_{g\infty}$) to achieve full cure. Our cure temperature of 180 °C is above $T_{g\infty}$ for all but our bulk system. However, because of the slow reaction and long reaction times for the uncatalyzed monomer studied, diffusion control after vitrification does not prohibit full cure from being achieved in this system.[39]

In order to determine the relationship between $T_g$ and conversion, we also measured both $T_g$ and the residual heat of reaction as a function of cure time with the conversion $x$ being determined from the residual heat of reaction:

$$x = \frac{\Delta H_T - \Delta H_r}{\Delta H_T} \qquad (5)$$

where $\Delta H_T$ is the total heat of reaction of an initially uncured sample (after 3 min imbibement) and $\Delta H_r$ is the residual heat of reaction for a partially cured sample. The monomer confined in the controlled pore glasses was cured at 180 °C for times ranging from 0 to 8 h. The residual heat of reaction and onset cure temperature were obtained upon scanning the partially cured sample to 380 °C at 10 K/min; the onset temperature of the cure exotherm is determined by the intersection of the baseline with a line drawn tangent to the steep part of the exotherm on the low-temperature side. After the scan to 380 °C, the sample is fully cured and a new sample is used for measurement of the residual heat at a different cure time. Figure 2a shows the evolution of the glass transition temperature and residual heat of reaction as a function of the cure time at 180 °C for the monomer confined within the 24.6 nm controlled pore glass after imbibition. As the cure time increases, the glass transition temperature increases and the residual heat of reaction decreases (i.e., the conversion increases from 0 to 1). We note that the glass transition temperature as a function of cure time is also obtained from this type of measurement, and the data are plotted together with those obtained from the first method in the results. Three replicates were used to obtain the total heat of reaction and onset cure temperature of the initially uncured monomer confined in the CPG at each pore size. Figure 2b shows the cure exotherm of initially uncured bisphenol M dicyanate ester at 10 K/min in the bulk state and confined in the 110.6 and 24.6 nm CPGs after imbibition at 100 °C for 3 min. It is clear that, although the heat of reaction is unchanged by nanoconfinement, the onset temperature shifts dramatically to lower temperatures with decreasing pore size.

The temperature of the DSC was calibrated with mercury and indium at 10 K/min on heating and was maintained at an accuracy of ±0.1 °C. The heat flow of the DSC was calibrated with indium.

## Results

**Glass Transition Temperature of Confined Bisphenol M Dicyanate Ester Monomer.** The glass transition temperatures

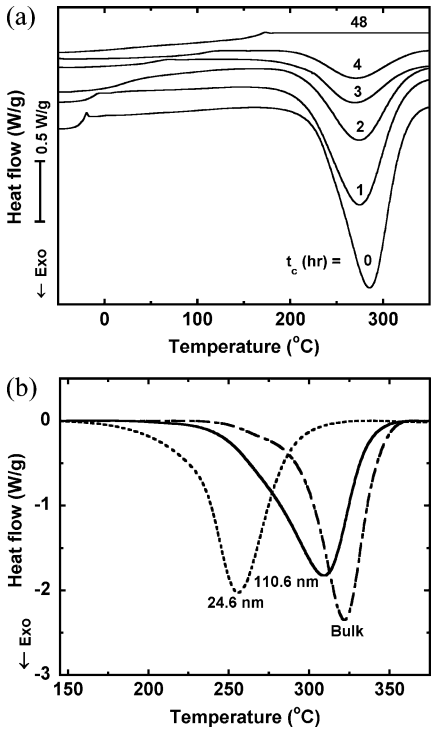


**Figure 2.** (a) DSC heating scans showing the evolution of glass transition temperature and residual heat of reaction of bisphenol M dicyanate ester confined in the controlled pore glass with pore size of 24.6 nm when cured at 180 °C for times ranging from 0 to 48 h after imbibition at 100 °C for 10 h. (b) DSC heating scans showing the heat of reaction for initially uncured bisphenol M dicyanate ester at 10 K/min in the bulk state and confined in the controlled pore glasses with pore size of 110.6 and 24.6 nm after imbibition at 100 °C for 3 min.

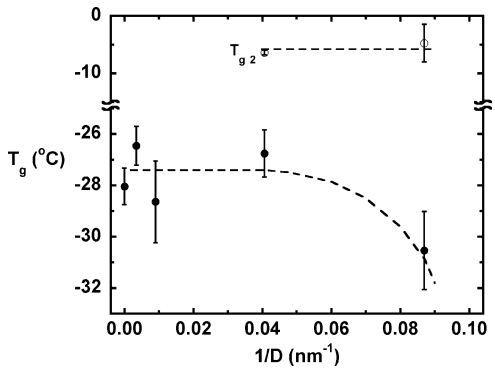


**Figure 3.** Glass transition temperature of bisphenol M dicyanate ester monomer in the bulk and nanoconfinement states. The solid symbols represent the primary $T_g$, and the open symbol represents the additional upper $T_g$s. The dashed lines are drawn to guide the eyes.

($T_g$) of the bisphenol M dicyanate ester monomer under nanoconfinement and in the bulk state are shown in Figure 3. A small $T_g$ depression of 3.4 K is observed for the monomer confined in the CPG with the smallest pore size of 11.5 nm. The presence of a confinement effect on the monomer $T_g$ indicates that the penetration of the monomer into the nanopores occurs within minutes at 100 °C, consistent with our estimate of imbibition time based on the model of Huber et al.[44]

One $T_g$ is present for the monomer confined in CPGs with pore sizes greater than 100 nm, whereas two $T_g$s are observed for those with pore sizes smaller than 25 nm. The second transition, $T_{g2}$, is ~22 K above the bulk value and is observed for the monomer confined in 24.6 and 11.5 nm pores. Secondary transitions have similarly been observed using DSC for polystyrene/*o*-terphenyl solutions confined in CPGs[4] as well as for

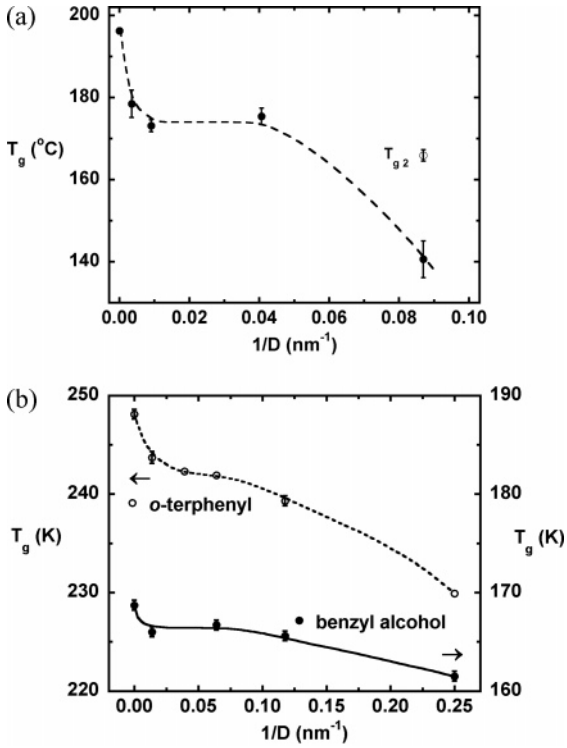


**Figure 4.** (a) Glass transition temperature depression for the polycyanurates under nanoconfinement. The solid symbols represent the primary $T_g$, and the open symbol represents the additional upper $T_g$. The dashed lines are drawn to guide the eyes. The data in the bulk state are from the previous study by Simon and Gillham[39] with a standard deviation of ±0.5 °C (too small to be seen in the figure). (b) Glass transition temperatures as a function of reciprocal pore diameter for nanoconfined polystyrene/*o*-terphenyl solutions, *o*-terphenyl, and benzyl alcohol, which were obtained by Park and McKenna[4] and Jackson and McKenna,[2,6] respectively; the data were refit by us.

propylene glycol confined in the silanized and unsilanized porous glasses;[58] secondary transitions have also been observed using dielectric measurements, solvation dynamics measurements, and light scattering studies for other small molecule glass formers.[59−69] The origin of the upper $T_g$ is generally ascribed to surface interactions, and this will be addressed further in the discussion.

**Glass Transition Temperature of Confined "Fully Cured" Polycyanurate.** Similar to the depression of the glass transition of the monomer by nanoconfinement, the $T_g$ of the "fully cured" polycyanurate also decreases with decreasing pore size, as shown in Figure 4a. However, the magnitude of the depression for the polymer is considerably greater, being 56 K at the smallest pore size of 11.5 nm. Our findings are consistent with those of Wang and Zhou, in which a 15 K depression in the glass transition temperature was observed for 40 nm microtome-sliced epoxy thin film;[11] we estimate a 25 K depression at a similar length scale from our work. Although these depressions are significantly greater than what is generally observed for small molecule glass formers confined to nanopores at the same pore size, they are still smaller than those observed for freely standing polymer films; for example, a 77 K depression in $T_g$ is observed for the freely standing, 63 nm thick, polystyrene ($M_w$ = 6 680 000 g/mol) film.[70] Furthermore, the $T_g$ depression of nanoconfined polycyanurates with pore size appears to be nonlinear, decreasing initially, then leveling off in the range of 100 to 25 nm, and decreasing again below 25 nm. This apparent nonlinear behavior is consistent with the experimental data on *o*-terphenyl (*o*-TP), benzyl alcohol, and polystyrene/*o*-terphenyl (PS/*o*-TP) solutions confined in silanized CPGs[2,4,6] upon our reanalysis

**Table 2. Total Heat of Reaction and Onset Cure Temperature of the Monomer under Nanoscale Constraints at Different Sizes**

| | mean pore diameter (nm) | | | | |
|---|---|---|---|---|---|
| | ∞ | 287.8 | 110.6 | 24.6 | 11.5 |
| $\Delta H$ (J/mol −OCN) | 110.0 ± 7.8 | 111.9 ± 1.2 | 111.4 ± 3.3 | 111.6 ± 2.9 | 113.2 ± 6.1 |
| $T_{onset}$ (°C) | 292.2 ± 1.0 | 247.3 ± 7.4 | 242.4 ± 2.3 | 217.3 ± 9.6 | 206.7 ± 20.3 |

of the literature data, as shown in Figure 4b. Alcoutlabi and McKenna also pointed out that the $T_g$ vs inverse pore diameter ($1/D$) of *o*-terphenyl confined in controlled pore glasses does not follow a strict linear relationship within the pore diameter investigated, although the data were originally plotted using a linear fit.[3] On the other hand, when only pore sizes below 15 nm are studied, linear relationships of $T_g$ vs inverse pore radius are observed as for the cases of isopropylbenzene, glycerol, di-*n*-butyl phthalate, *tert*-butylbenzene, and *n*-butyl acetate confined in porous silica glasses;[5] the apparent linearity in these cases may be the result of the narrow pore size range investigated.

For the "fully cured" polycyanurate confined in the 11.5 nm CPG, a second upper transition, $T_{g2}$, appears around 23 K above the primary $T_g$ but still below the bulk $T_g$ of the unconfined material. On the other hand, the second transition is not observed for the polycyanurate network confined in the 24.6 nm CPG pores, although it was observed for the monomer confined to this pore size.

The depression of the final glass transition temperatures of polycyanurate networks under nanoscale constraint observed in the current study corroborates that the BMDC monomer does penetrate into the nanopores instead of acting as fillers because the glass transition temperature of the polymer is not expected to be affected by micrometer-sized particles (such as these CPGs, whose particle sizes are 74−125 $\mu$m); for example, no $T_g$ depression is observed for epoxy/silica[16] and PMMA/alumina composites[71] having micrometer-sized particles. Furthermore, the observed glass transition temperature depression of polycyanurate networks confined in the controlled pore glasses is not because of incomplete curing; rather, it is due to the nanoconfinement effect. The full conversion of the monomer under nanoconfinement is evidenced by the fact that the total heat of reaction (measured for the initially uncured systems after 3 min imbibement) is constant independent of pore size, as shown in Table 2. Full conversion of the monomer is further corroborated by the disappearance of cyanate functional groups in the FTIR spectra of monomer cured in an alumina nanofilter having 100 nm pores (not shown). The full conversion of the monomer under nanoconfinement suggests that the chemical structure of the network is not affected by nanoconfinement; however, our result is in contrast to the finding from Kim and Torkelson, which shows that nanoconfinement reduces the physical cross-linking and network formation in a telechelic, pyrene-labeled poly(dimethylsiloxane) thin film system.[72]

**Effect of Pore Size on the Cure Kinetics of Bisphenol M Dicyanate Ester.** The cure kinetics of bisphenol M dicyanate ester confined in the controlled pore glasses is investigated by following the evolution of the glass transition temperature during cure. The results are shown in Figure 5 as a function nanopore size. As the pore size decreases from infinity (i.e., the bulk state) to 11.5 nm, cure is significantly accelerated. It has been suggested that the enhanced reactivity observed at the nanoscale in this system may be attributed to the increased collision efficiency of the molecules in the vicinity of the surface due to decreased mobility (i.e., due to reduced degrees of freedom).[73] The accelerated cure under nanoconfinement is also corroborated by the fact that the DSC onset temperature for the reaction of initially uncured monomer confined in the CPGs decreases as pore size decreases, as tabulated in Table 2 and as shown in Figure 2b. Furthermore, on the basis of the similarity found for the nanocomposites and ultrathin film as discussed in the Introduction,[34−37] this observation may be analogous to the curing of epoxy resin in the presence of carbon nanotubes where the reaction rate is found to increase with increasing nanotube loading (i.e., with decreasing interparticle spacing),[25] although our finding is contrary to the result from epoxy/SiC nanocomposites, which shows a delayed cure reaction of epoxy with the incorporation of SiC.[13] It must be noted, however, that catalytic (or reaction inhibiting) groups on surfaces could be more important than the effects associated with reduced degrees of freedom at the surface. Additionally, Figure 5 also shows that the material associated with the second (higher) $T_g$ cures faster than that associated with the primary $T_g$ in the smallest CPG of 11.5 nm.

The evolution of the glass transition temperature $T_g$ can be described using the cure kinetics model discussed in the Introduction, i.e., eqs 1 and 2. To account for the acceleration of cure in the nanopores, we assume that both the second-order and second-order autocatalytic reactions are modified in a similar way:

$$\frac{dx}{dt} = \alpha k(1 - x)^2(x + b) \tag{6}$$

where $\alpha$ is the acceleration factor, i.e., the ratio of the rate constant under nanoconfinement to that in the bulk state, and the other parameters are considered to have the same values as reported[39] for the bulk (unconfined) BMDC resin. The model, shown in Figure 5 as solid lines, describes the experimental data well. The acceleration factor is plotted against the inverse pore diameter ($1/D$) in Figure 6 and increases with decreasing pore diameter as expected. The monomer cures 7.5 times faster within the smallest pore of 11.5 nm relative to the bulk. Furthermore, the acceleration factor is even greater for the material associated with $T_{g2}$, which exhibits an acceleration factor of 11.

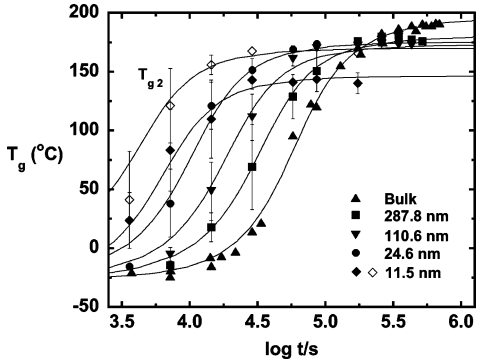


**Figure 5.** Effect of pore size of controlled pore glass on the evolution of glass transition temperature of bisphenol M dicyanate ester during curing process. The solid symbols represent the primary $T_g$, and the open symbol represents the additional upper $T_g$. The solid lines are the fits to the cure kinetic model. Part of the data in the bulk state are from the previous study by Simon and Gillham.[39] For the data at cure times of 4 h or shorter, the error bars are based on at least three replicates, whereas for the data at cure times of 8 h or longer, the error bars are based on at least two replicates.

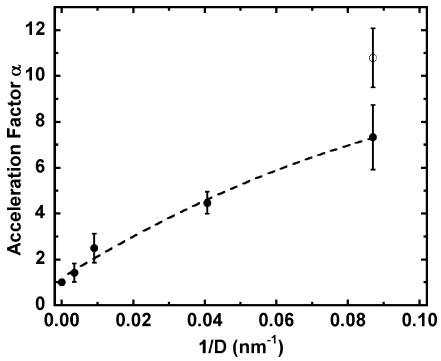


**Figure 6.** Acceleration factor α, the ratio of the rate constant under nanoconfinement to that in the bulk state, as a function of inverse pore diameter. The solid symbols represent the acceleration factor associated with the primary $T_g$, and the open symbol represents the one associated with the additional upper $T_g$. The dashed lines are drawn to guide the eyes.

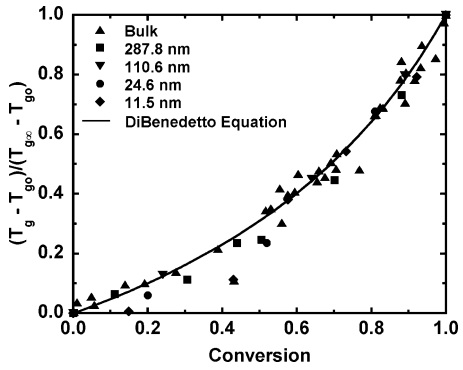


**Figure 7.** Relative glass transition temperature as a function of conversion. Solid line represents the DiBenedetto equation. The data in the bulk state are from the previous study by Simon and Gillham.[39]

The relationship between the dimensionless glass transition temperature, $T_g^* = (T_g - T_{g0})/(T_{g\infty} - T_{g0})$, and the conversion for the bisphenol M dicyanate ester cured under nanoconfinement and in the bulk state is plotted in Figure 7. The dimensionless $T_g^*$ is independent of pore size, and all the data collapse onto a single cure, which can be described by the DiBenedetto equation,[40] eq 2. The best fit value of $\lambda$ for the nanoconfined resin is 0.45 with a standard deviation of 0.02, consistent with the value of 0.426 previously reported[39] for the bulk. We note that this relationship was used in conjunction with eq 6 to model the $T_g$ vs time data shown in Figure 5. Furthermore, we suggest that the fact that the dimensionless glass transition temperature vs conversion relationship is independent of pore size implies that the network structure is unchanged upon nanoconfinement. This issue will be further elaborated on in the following discussion.

## Discussion

**Origin of the Upper $T_g$, the Associated Length Scale, and Implications.** As observed in the Results section, besides the primary glass transition, an additional relaxation at higher temperature, $T_{g2}$, appears for the monomer confined in the 24.6 and 11.5 nm CPGs and polycyanurate in the 11.5 nm CPG. Such an additional relaxation has been observed in calorimetric studies,[4,58] dielectric studies,[59−67] dynamic light scattering study,[68] and solvation dynamics measurements[69] of small molecular weight glass formers confined in both silanized[4,58] and unsilanized[58−69] pores at small pore sizes. A two-layer model, which consists of a core and a less mobile surface layer,[59] is often applied to describe the two glass transitions or relaxations of glass formers under nanoconfinement. The upper glass transition or slower relaxation has been attributed to the formation of a less mobile surface layer by physically or chemically trapped molecules which can be promoted in smaller pores.[4,58−69] A length scale for this layer can be determined assuming that the heat capacity changes at the primary and secondary glass transitions are proportional to the number of molecules associated with each transition and that the pores in the CPGs are cylindrical:[4]

**Table 3. Length Scale Associated with the Additional $T_g$ for the Monomer and Polycyanurate under Nanoconfinement[a]**

| *d* (nm) for bisphenol M dicyanate ester monomer | *d* (nm) for polycyanurate |
|---|---|
| 0.57 ± 0.12 | 1.58 ± 0.69 |

[a] The calculation assumes cylindrical pores for all the CPGs and that the thickness of the silane layer is 0.1 nm[43] in the silanized CPGs.

$$\frac{\Delta C_{p,2}}{\Delta C_{p,T}} = \frac{\pi[r^2 - (r-d)^2]}{\pi r^2} \tag{7}$$

where $\Delta C_{p,2}$ is the heat capacity change at glass transition associated with the upper $T_g$, $\Delta C_{p,T}$ is the total heat capacity change at glass transition associated with both the primary and the upper $T_g$, $r$ is the pore radius of the CPG, and $d$ is the length scale associated with the upper $T_g$. The length scales for both monomer and polycyanurate under nanoconfinement are listed in Table 3. The length scale associated with the upper $T_g$ is 0.57 ± 0.12 nm for the monomer and is 1.58 ± 0.69 nm for the "fully cured" polycyanurate. Comparable length scales ranging from 0.9 to 0.3 nm have been reported for hydrogen-bonded liquids such as propylene glycol, butylene glycol, and pentylene glycol confined in unsilanized CPGs with pore sizes of 2.5−7.5 nm when analyzed using a three-layer model.[74] Even smaller length scales, 0.09 and 0.13 nm, were obtained for propylene glycol confined in silanized and unsilanized nanoporous glasses, respectively, with pore size ranging from 5.0 to 2.5 nm using a two-layer model.[58] However, longer length scales, more in line with those for the nanoconfined polycyanurates, have also been determined to range from 0.96 to 2.5 nm as the pore diameter increases from 11.6 to 47.9 nm for polystyrene/*o*-terphenyl solutions in silanized CPGs.[4] Nevertheless, the observation of glass transition behavior for length scales shorter than that associated with cooperativity, which is generally assumed to be a few nanometers,[75] for the monomeric small molecule glass formers investigated in the current study and for other small molecules reported in the literature is difficult to fully explain.

***$T_g$* Depression for "Fully Cured" Polycyanurates under Nanoconfinement—Intrinsic Size Effect?** The observed glass transition temperature depression of polycyanurate networks confined in the controlled pore glasses could be caused by several factors: (1) intrinsic size effect, (2) incomplete cure, (3) negative pressure development due to cure shrinkage, and (4) a higher degree of side reaction resulting in a reduced cross-link density under nanoconfinement. The $T_g$ depression is not due to incomplete curing as already discussed and as evidenced by the invariance of the total heat of reaction of the monomer under nanoconfinement with pore size (shown in Table 2). Additionally, the negative pressure developed upon cure in 3-D confinement due to the cure shrinkage is not expected to cause the $T_g$ depression. In other work, the tensile stresses at the end of cure for an epoxy resin confined to macroscopic 3-D constraint (in an open strain-gauged tube) ranged from 0 to 7

MPa as a result of the network chemical relaxation in the gel;[76] given that the pressure dependence of glass transition temperature ($dT_g/dP$) for a similar high $T_g$ epoxy system is 0.23 K/MPa,[77] the result is a $T_g$ depression of less than 2 K. In addition, any depression in $T_g$ resulting from negative pressure effect might not be expected to depend strongly on pore size, which is not the observation. Concerning the effect of side reactions, monomer intracyclization has recently been discovered to contribute to the delayed gelation of bisphenol M dicyanate ester and other cyanate esters with similar structures, and it occurs with a probability of 14% in bulk bisphenol M dicyanate ester.[41] At the current stage, how the nanoconfinement influences the probability of occurrence of monomer intracyclization is unknown. Nevertheless, as indicated in our previous study,[41] the probability of monomer intracyclization increases when the two functional groups on a single monomer are more easily accessed such as for the monomers with moderately long and flexible backbone chains or when those from other monomers are less likely to be accessed, for instance in a more diluted monomer solution.[78] Under nanoscale constraint, the probability for one functional group to access the other one from its own molecule is not expected to exceed that in the bulk state because the molecules may be expected to have fewer degrees of freedom similar to polymer thin films;[79] consequently, monomer intracyclization is not expected to be more probable than in the bulk. Furthermore, the unchanged network structure under nanoconfinement as implied by the invariant $T_g$ vs conversion relationship (Figure 7) indicates that the side reaction under nanoconfinement occurs to a similar degree as in the bulk state. On the basis of these arguments, we suggest that the magnitude of the depression in the glass transition temperature of polycyanurate networks under nanoscale constraint is attributable to an intrinsic size effect. However, experiments are underway to quantify the role of monomer intracyclization at the nanoscale.

## Conclusions

The influence of nanoscale confinement on the glass transition and the isothermal curing behavior of bisphenol M dicyanate ester is studied. Glass transition temperature depressions of only a few degrees are observed for the confined monomer, but depressions of up to 56 K are observed for polycyanurate networks confined in the 11.5 nm diameter controlled pore glass. The $T_g$ depression appears to be a nonlinear function of inverse pore diameter. Nanoscale constraint strongly accelerates the cure of bisphenol M dicyanate ester, and the acceleration factor increases with decreasing pore size. The heat of reaction and dimensionless $T_g$ vs conversion relationship is unchanged for the material cured in the nanopores, indicating complete cure with no change in the network structure. Two $T_g$s are observed for the monomer confined in the controlled pore glasses at 24.6 and 11.5 nm, whereas the second $T_g$ is not observed for the polycyanurate networks confined in the 24.6 nm controlled pore glass. Assuming the second $T_g$ reflects the less-mobile surface layer in a two-layer model, the length scale for the additional $T_g$ ranges from 0.57 to 1.58 nm, the lower bound of which is less than the generally accepted length scale for cooperativity.

**Acknowledgment.** We acknowledge the American Chemical Society Petroleum Research Fund Grant 45416-AC7 for their financial support of this project. The donation of part of the controlled pore glasses from Millipore is also gratefully acknowledged. We also thank Professor Sergey Vyazovkin from University of Alabama at Birmingham for his thoughtful comments on this work. The help on contact angle measurement from Professor Lenore L. Dai at Texas Tech University is also gratefully acknowledged.

## References and Notes

(1) Jackson, C. L.; McKenna, G. B. *J. Chem. Phys.* **1990**, *93*, 9002.
(2) Jackson, C. L.; McKenna, G. B. *J. Non-Cryst. Solids* **1991**, *221*, 131−133.
(3) Alcoutlabi, M.; McKenna, G. B. *J. Phys.: Condens. Matter* **2005**, *17*, R461.
(4) Park, J.-Y.; McKenna, G. B. *Phys. Rev. B* **2000**, *61*, 6667.
(5) Zhang, J.; Liu, G.; Jonas, J. *J. Phys. Chem.* **1992**, *96*, 3478.
(6) Jackson, C. L.; McKenna, G. B. *Chem. Mater.* **1996**, *8*, 2128.
(7) Sharp, J. S.; Teichroeb, J. H.; Forrest, J. A. *Eur. Phys. J. E* **2004**, *15*, 473.
(8) Fakhraai, Z.; Sharp, J. S.; Forrest, J. A. *J. Polym. Sci., Part B: Polym. Phys.* **2004**, *42*, 4503.
(9) Christenson, H. K. *J. Phys.: Condens. Matter* **2001**, *13*, R95.
(10) Alba-Simionesco, C.; Coasne, B.; Dosseh, G.; Dudziak, G.; Gubbins, K. E.; Radhakrishnan, R.; Sliwinska-Bartkowiak, M. *J. Phys.: Condens. Matter* **2006**, *18*, R15.
(11) Wang, X.; Zhou, W. *Macromolecules* **2002**, *35*, 6747.
(12) Dinakaran, K.; Alagar, M. *Polym. Adv. Technol.* **2003**, *14*, 574.
(13) Zhou, T.; Gu, M.; Jin, Y.; Wang, J. *Polymer* **2005**, *46*, 6216.
(14) Zhou, T.; Gu, M.; Jin, Y.; Wang, J. *Polymer* **2005**, *46*, 6174.
(15) Zhou, T.; Gu, M.; Jin, Y.; Wang, J. *J. Polym. Sci., Part A: Polym. Chem.* **2006**, *44*, 371.
(16) Sun, Y.; Zhang, Z.; Moon, K.-S.; Wong, C. P. *J. Polym. Sci., Part B: Polym. Phys.* **2004**, *42*, 3849.
(17) Lee, T.-M.; Ma, C.-C. M. *J. Polym. Sci., Part A: Polym. Chem.* **2006**, *44*, 757.
(18) Kornmann, X.; Thomann, R.; Mulhaupt, R.; Finter, J.; Berglund, L. A. *Polym. Eng. Sci.* **2002**, *42*, 1815.
(19) Kornmann, X.; Thomann, R.; Mulhaupt, R.; Finter, J.; Berglund, L. A. *J. Appl. Polym. Sci.* **2002**, *86*, 2643.
(20) Mondragon, I.; Solar, L.; Nohales, A.; Vallo, C. I.; Gomez, C. M. *Polymer* **2006**, *47*, 3401.
(21) Triantafillidis, C. S.; LeBaron, P. C.; Pinnavaia, T. J. *J. Solid State Chem.* **2002**, *167*, 354.
(22) Miyagawa, H.; Rich, M. J.; Drzal, L. T. *J. Polym. Sci., Part B: Polym. Phys.* **2004**, *42*, 4384.
(23) Miyagawa, H.; Rich, M. J.; Drzal, L. T. *J. Polym. Sci., Part B: Polym. Phys.* **2004**, *42*, 4391.
(24) Ganguli, S.; Dean, D.; Jordan, K.; Price, G.; Vaia, R. *Polymer* **2003**, *44*, 1315.
(25) Xie, H.; Liu, B.; Yuan, Z.; Shen, J.; Cheng, R. *J. Polym. Sci., Part B: Polym. Phys.* **2004**, *42*, 3701.
(26) Schadler, L. S.; Giannaris, S. C.; Ajayan, P. M. *Appl. Phys. Lett.* **1998**, *73*, 3842.
(27) Bryning, M. B.; Islam, M. F.; Kikkawa, J. M.; Yodh, A. G. *Adv. Mater.* **2005**, *17*, 1186.
(28) Bryning, M. B.; Milkie, D. E.; Islam, M. F.; Kikkawa, J. M.; Yodh, A. G. *Appl. Phys. Lett.* **2005**, *87*, 161909.
(29) Zhu, J.; Kim, J.; Peng, H.; Margrave, J. L.; Khabashesku, V. N.; Barrera, E. V. *Nano Lett.* **2003**, *3*, 1107.
(30) Zhu, J.; Peng, H.; Rodriguez-Macias, F.; Margrave, J. L.; Khabashesku, V. N.; Imam, A. M.; Lozano, K.; Barrera, E. V. *Adv. Funct. Mater.* **2004**, *14*, 643.
(31) Gong, X.; Liu, J.; Baskaran, S.; Voise, R. D.; Young, J. S. *Chem. Mater.* **2000**, *12*, 1049.
(32) Ajayan, P. M.; Scchadler, L. S.; Giannaris, C.; Rubio, A. *Adv. Mater.* **2000**, *12*, 750.
(33) Moniruzzaman, M.; Winey, K. I. *Macromolecules* **2006**, *39*, 5194.
(34) Starr, F. W.; Schroder, T. B.; Glotzer, S. C. *Phys. Rev. E* **2001**, *64*, 021802.
(35) Bansal, A.; Yang, H.; Li, C.; Cho, K.; Benicewicz, B. C.; Kumar, S. K.; Schadler, L. S. *Nat. Mater.* **2005**, *4*, 693.
(36) Bansal, A.; Yang, H.; Li, C.; Benicewicz, B. C.; Kumar, S. K.; Schadler, L. S. *J. Polym. Sci., Part B: Polym. Phys.* **2006**, *44*, 2944.
(37) Rittigstein, P.; Torkelson, J. M. *J. Polym. Sci., Part B: Polym. Phys.* **2006**, *44*, 2935.
(38) Shimp, D. A. Technologically driven applications for cyanate resins. In *Chemistry and Technology of Cyanate Ester Resins*; Hamerton, I., Ed.; Blackie Academic & Professional: London, 1994.
(39) Simon, S. L.; Gillham, J. K. *J. Appl. Polym. Sci.* **1993**, *47*, 461.
(40) Nielsen, L. E. *J. Macromol. Sci., Rev. Macromol. Chem.* **1969**, *C3*, 69.
(41) Li, Q. X.; Simon, S. L. *Macromolecules* **2007**, *40*, 2246.
(42) Snow, A. W. The synthesis, manufacture and characterization of cyanate ester monomers. In *Chemistry and Technology of Cyanate Ester Resins*; Hamerton, I., Ed.; Blackie Academic & Professional: London, 1994.

(43) Erb, V. Diploma Thesis, Max-Planck-Institut fur Polymerforschung, Mainz, 1993.
(44) Huber, P.; Gruner, S.; Schafer, C.; Knorr, K.; Kityk, A. V. *Eur. Phys. J. Spec. Top.* **2007**, *141*, 101.
(45) Snow, A. W.; Buckley, L. J. *Macromolecules* **1997**, *30*, 394.
(46) Hodzic, A.; Stachurski, Z. H. *Compos. Interfaces* **2001**, *8*, 415.
(47) Page, S. A.; Berg, J. C.; Manson, J.-A. E. *J. Adhesion Sci. Technol.* **2001**, *15*, 153.
(48) Synytska, A.; Michel, S.; Pleul, D.; Bellmann, C.; Schinner, R.; Eichhorn, K.-J.; Grundke, K. *J. Adhes.* **2004**, *80*, 667.
(49) Small, D. *The Physical Chemistry of Lipids*; Plenum Press: New York, 1986.
(50) Williams, M. L.; Landel, R. F.; Ferry, J. D. *J. Am. Chem. Soc.* **1955**, *77*, 3701.
(51) Sze, H. P.; Pasiah, I. J.; Chew, G. In *Correlation of Underfill Viscosity and Contact Angle on Surfaces in a Flip Chip Package*; Electronics Packaging Technology Conference; Beng, L. T., Lee, C., Chuan, T., Eds.; Institute of Electrical and Electronics Engineers: Singapore, 2000; p 186.
(52) Debolt, M. A.; Easteal, A. J.; Macedo, P. B.; Moynihan, C. T. *J. Am Ceram. Soc.* **1976**, *59*, 16.
(53) Moynihan, C. T.; Macedo, P. B.; Montrose, C. J.; Gupta, P. K.; DeBolt, M. A.; Dill, J. F.; Dom, B. E.; Drake, P. W.; Easteal, A. J.; Elterman, P. B.; Moeller, R. P.; Sasabe, H.; Wilder, J. A. *Ann. N.Y. Acad. Sci.* **1976**, *279*, 15.
(54) Badrinarayanan, P.; Zheng, W.; Li, Q.; Simon, S. L. *J. Non-Cryst. Solids* **2007**, *353*, 2603.
(55) Moynihan, C. T.; Easteal, A. J.; DeBolt, M. A.; Tucker, J. *J. Am. Ceram. Soc.* **1976**, *59*, 12.
(56) Plazek, D. J.; Frund, Z. N. *J. Polym. Sci., Part B: Polym. Phys.* **1990**, *28*, 431.
(57) Hempel, E.; Huwe, A.; Otto, K.; Janowski, F.; Schröter, K.; Donth, E. *Thermochim. Acta* **1999**, *337*, 163.
(58) Zheng, W.; Simon, S. L. *J. Chem. Phys.* **2007**, *127*, 194501.
(59) Arndt, M.; Stannarius, R.; Gorbatschow, W.; Kremer, F. *Phys. Rev. E* **1996**, *54*, 5377.
(60) Arndt, M.; Stannarius, R.; Groothues, H.; Hempel, E.; Kremer, F. *Phys. Rev. Lett.* **1997**, *79*, 2077.
(61) Barut, G.; Pissis, P.; Pelster, R.; Nimtz, G. *Phys. Rev. Lett.* **1998**, *80*, 3543.
(62) Mel'nichenko, Y. B.; Schüller, J.; Richert, R.; Ewen, B.; Loong, C.-K. *J. Chem. Phys.* **1995**, *103*, 2016.
(63) Pissis, P.; Kyritsis, A.; Barut, G.; Pelster, R.; Nimtz, G. *J. Non-Cryst. Solids* **1998**, *444*, 235−237.
(64) Pissis, P.; Kyritsis, A.; Daoukaki, D.; Barut, G.; Pelster, R.; Nimtz, G. *J. Phys.: Condens. Matter* **1998**, *10*, 6205.
(65) Schönhals, A.; Goering, H.; Schick, C.; Frick, B.; Zorn, R. *Colloid Polym. Sci.* **2004**, *282*, 882.
(66) Schüller, J.; Mel'nichenko, Y. B.; Richert, R.; Fischer, E. W. *Phys. Rev. Lett.* **1994**, *73*, 2224.
(67) Schüller, J.; Richert, R.; Fischer, E. W. *Phys. Rev. B* **1995**, *52*, 15232.
(68) Patkowski, A.; Ruths, T.; Fischer, E. W. *Phys. Rev. E* **2003**, *67*, 021501.
(69) Streck, C.; Mel'nichenko, Y. B.; Richert, R. *Phys. Rev. B* **1996**, *53*, 5341.
(70) Dalnoki-Veress, K.; Forrest, J. A.; Murray, C.; Gigault, C.; Dutcher, J. R. *Phys. Rev. E* **2002**, *63*, 031801.
(71) Ash, B. J.; Rogers, D. F.; Wiegand, C. J.; Schadler, L. S.; Siegel, R. W.; Benicewicz, B. C.; Apple, T. *Polym. Compos.* **2002**, *23*, 1014.
(72) Kim, S. D.; Torkelson, J. M. *Macromolecules* **2002**, *35*, 5943.
(73) Private communication with Professor Sergey Vyazovkin from University of Alabama at Birmingham.
(74) Gorbatschow, W.; Arndt, M.; Stannarius, R.; Kremer, F. *Europhys. Lett.* **1996**, *35*, 719.
(75) Donth, E. *Relaxation and Thermodynamics in Polymers*; Akademie Verlag: Berlin, 1992.
(76) Merzlyakov, M.; McKenna, G. B.; Simon, S. L. *Composites, Part A* **2006**, *37*, 589.
(77) Warfield, R. W. *Makromol. Chem.* **1968**, *116*, 78.
(78) Korshak, V. V.; Pankratov, V. A.; Ladovskaya, A. A.; Vinogradova, A. V. *J. Polym. Sci., Part A: Polym. Chem.* **1978**, *16*, 1697.
(79) Koh, Y. P.; McKenna, G. B.; Simon, S. L. *J. Polym. Sci., Part B: Polym. Phys.* **2006**, *44*, 3518.

MA702144B